DE GRUYTER OPEN

Archives of Hydro-Engineering and Environmental Mechanics
Vol. 63 (2016), No. 2–3, pp. 101–120
DOI: 10.1515/heem-2016-0007

The Effect of the Vertical Acceleration on Stability Assessment of Seismically Loaded Earth Dams

Aleksandra Korzec

Institute of Hydro-Engineering, Polish Academy of Sciences, ul. Kościerska 7, 80-328 Gdańsk, Poland,
e-mail: a.korzec@ibwpan.gda.pl

(Received October 06, 2016; revised December 14, 2016)

Abstract

In the assessment of slope stability, the vertical component of acceleration is commonly neglected. However, signal analyses performed on a large number of acceleration time histories have revealed that the vertical peak ground acceleration can be as high as the horizontal one. In this paper, a method of slope stability analysis regarding the vertical component of acceleration is proposed. It considers a rigid body system affected by the acceleration time histories in both horizontal and vertical directions. In a general case, the strength of the contact between acceleration components is time dependent. Parametric analysis was performed on the basis of cyclic harmonic loading, assuming a safety criterion in the form of permanent displacement. The results, for both harmonic and real acceleration time histories, were compared with the results of the commonly used Newmark's sliding block approach, which revealed significant differences in permanent displacements calculated by the two methods.

Key words: slope stability analysis; dynamics; Newmark's method; accelerogram

List of symbols

$a(t)$	–	block acceleration time-history acting, direction given in subscript, [m/s^2];
a_c	–	yield acceleration, block acceleration threshold, [m/s^2];
A	–	amplitude of subsoil acceleration, direction given in subscript, [m/s^2];
$A(t)$	–	subsoil/ground acceleration time-history, direction given in subscript, [m/s^2];
D	–	permanent displacement of the block, [m];
f	–	motion frequency, [Hz];
F	–	magnitude of inertia force, direction given in subscript, [kN];
FS	–	factor of safety, [–];
g	–	gravity acceleration, equal around 9.807 m/s^2;
N	–	static normal force, [kN];

m_b – mass of the block, [kg];
PHA – peak horizontal ground acceleration, [m/s^2];
(s, n) – local co-ordinate system;
$S, S(t)$ – shear resistance, [kN];
T – static shear force, [kN];
u_s – block displacement along slip plane, [m];
$u_{s,rel}$ – relative block displacement along slip plane, [m];
v_s – block velocity along slip plane, [m/s];
α – inclination angle, [°];
θ – phase angle, [–];
μ – friction coefficient, [–];
μ_k – kinetic friction coefficient, [–];
μ_s – static friction coefficient, [–].

1. Introduction

The stability assessment of an earth dam in the case of static loading is quite straightforward, and the methodology is well recognized and accepted, (Duncan 1996). However, dams can also be affected by dynamic loading coming from natural earthquakes or induced by mining operations. In that case, there are many more factors which should be considered starting from the selection of dynamic loading descriptors (e.g. peak value, Arias intensity, time history and its frequency range), dynamic properties of the material and ending with the formulation of a specific stability criterion (e.g. factor of safety, permanent displacement or root mean square value).

There are three main groups of stability assessment methods in case of dynamic loading (Eurocode 8 2004): the pseudo-static method (Terzaghi 1950), the permanent displacement approach (Newmark 1965) and the stress-deformation analysis (Clough and Chopra 1966). All these approaches have a number of advantages and limitations. A comprehensive review of these features can be found in papers by Day (2002), Kramer (1996), Sica et al (2002), Jibson (2011), Świdziński and Korzec (2015b). The simplest approach, the pseudo-static limit equilibrium method, strongly depends on the seismic coefficient assumed (Hynes-Griffin and Franklin 1984, Wieland 2008) and tells nothing about possible displacements. On the opposite side of the spectrum are stress-deformation analyses. The calculations are based on a discrete method, such as the finite element method, which makes it possible to take into account the stress-strain behaviour of soils (Ishibashi and Zhang 1993, Ishihara 2003) and to observe the response of the structure during shaking. These advantages, however, generate a number of disadvantages, such as the additional costs of time-consuming problem formulation and description of sophisticated material properties, increased computational effort and, last but not least, the increased time and effort for the interpretation of the results (Amorosi et al 2010, Dulińska 2012). The sliding block approach, presented by Newmark (1965) and then developed by Ambraseys and Sarma (1967)

fills the gap between the above-mentioned methods. It seems to be the most attractive and practical because it takes into account the acceleration time history, maintaining a simple measure of stability (Dobry 2014). This approach has been widely used in many predictive models, see papers by Jibson (1993), Romero (2000), Bray and Travasarou (2007). In addition, the restrictions of the original concept can be quite easily overcome, (Ambraseys and Sarma 1967, Biondi et al 2002, GEO-SLOPE 2010, Qi and Liu 2015). The most important development seems to be the assumption regarding the average acceleration proposed by Makdisi and Seed (1978), which makes it possible to couple this simple approach with stress-deformation analyses (Feng and Tsai 2010, Świdziński and Korzec 2015a). Let us look more closely at the classic sliding block approach.

In 1965, Newmark (1965) proposed a new criterion, called permanent displacement, to assess slope stability. For simplicity, the sliding block model is used to represent a sliding mass on an arbitrary embankment, Fig. 1. Newmark's sliding block approach assumes a temporary instability of the rigid block during shaking, which is expressed by yield acceleration a_c. The value of a_c corresponds to the inertia force that overcomes the interface resistance to downward sliding and hence to the pseudo-static factor of safety equal to 1. When earthquake acceleration $A_s(t)$ acting upwards exceeds a_c, downward sliding occurs. First, the velocity time history of the block is calculated by integrating the part of acceleration that exceed a_c (continuing until the zero speed), and then this velocity time history is integrated to obtain the cumulative permanent displacement after shaking. The numerical example is shown in Section 2.4. It is worth noting that sliding is induced only by the tangent component of acceleration, and the shear strength of the interface comes from the static normal component of the block weight, only.

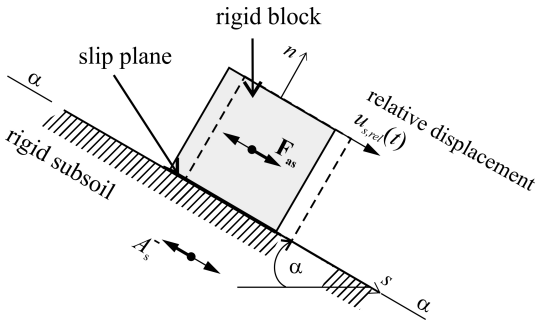

Fig. 1. Newmark's sliding block approach.

However, the structures are loaded by a combination of longitudinal and transverse motions coming from both material waves (S- and P-waves) and surface waves (Rayleigh, Love waves). Signal analyses performed on a wide group of acceleration time histories registered near the epicentres of mining-induced tremors have revealed

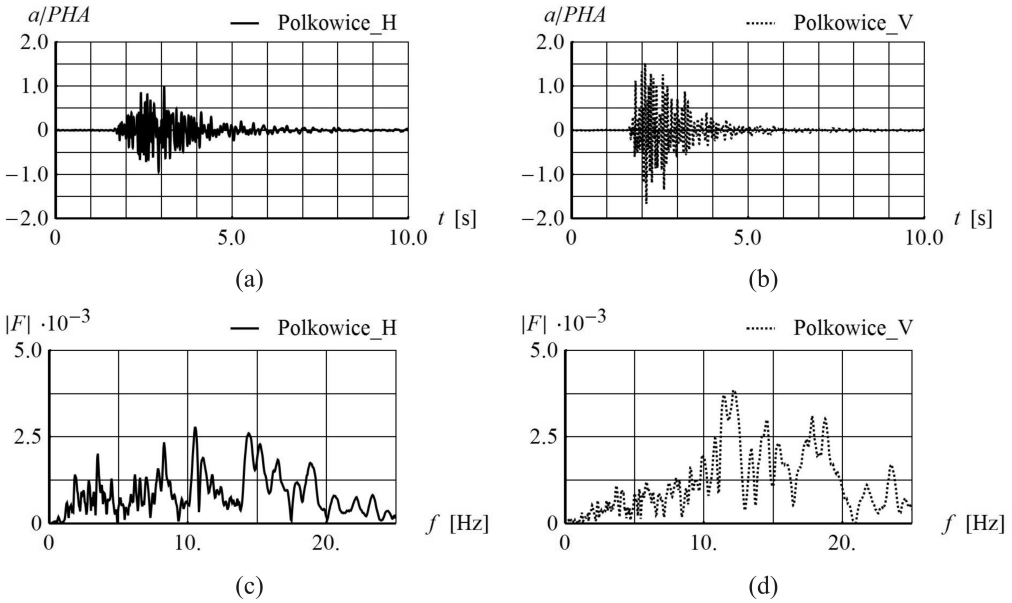

Fig. 2. Time histories of (a) horizontal – H and (b) vertical – V acceleration components registered in Polkowice, Poland, at a distance of 2 km from the epicentre of a 3 local magnitude mining-induced earthquake in 2002, (c), (d) their respective Fourier acceleration spectra.

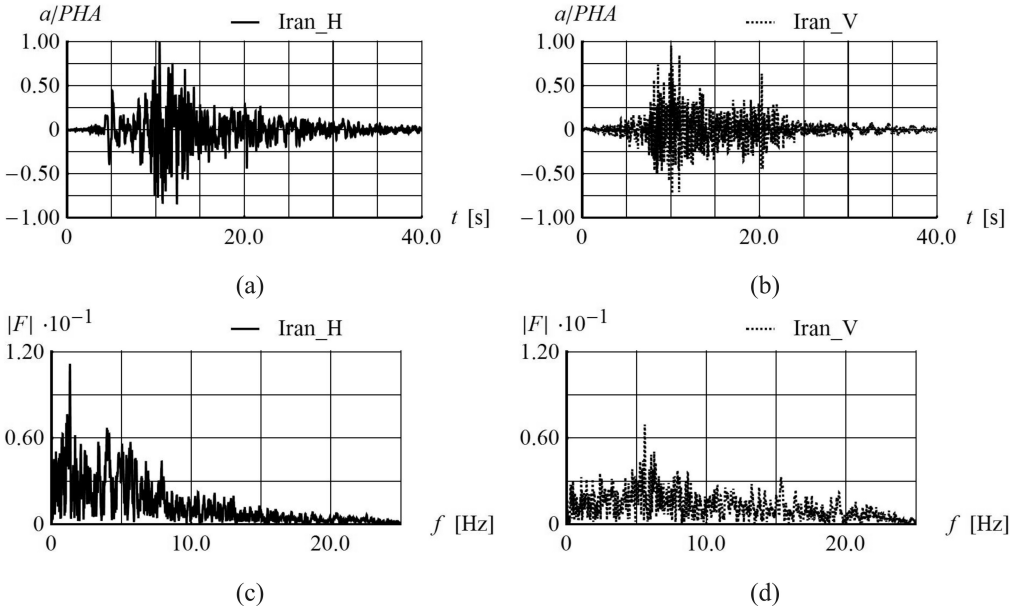

Fig. 3. Time histories of (a) horizontal – H and (b) vertical – V acceleration components registered at a distance of 57 km from the Tabas earthquake epicenter, Iran, 1998 (c), (d) their respective Fourier acceleration spectra.

that the vertical peak ground acceleration can be as high as or even higher than the horizontal one. Sample acceleration time histories and their Fourier acceleration spectra are shown in Fig. 2. Moreover, analyses performed on a group of natural earthquake records downloaded from the *European Strong-motion Database* (2015) have shown that this is true even for greater distances, for example, 57 km, shown in Fig. 3.

Commonly, after Newmark's work, it is assumed that the accelerations act only in the slip plane (Gazetas et al 2009, Sawicki and Chybicki 2005). Acceleration, on the other hand is calculated based on horizontal and vertical accelerations, but most often based solely on the horizontal aspect. However, the strong influence of vertical acceleration on quay-wall horizontal permanent displacement was proved by Sawicki et al (2007). Effects of vertical acceleration on a permanent displacement of slope using Newmark's method had been studied by Sarma and Scorer (2009), though the results of those calculations did not give an unambiguous answer to the question.

In the present paper, the impact of the vertical acceleration component on permanent displacement is examined on the basis of the dynamic equilibrium of the sliding block for vertical and horizontal accelerations acting simultaneously. With the use of this model a parametric study of the input motion is performed.

The paper is organised as follows. First, in Section 2, a specific case of acceleration is considered in order to compare the results of the proposed method and Newmark's method. The block motion solving routine is also presented. Further, in Section 3, the equilibrium equations are derived for both components of accelerations. The results of the parametric study are discussed in Section 4. Finally, the conclusions are given in Section 5.

2. Simple Rigid Block Case

2.1. Limit Equilibrium Equation

Let us consider a very simple system of two rigid bodies, consisting of a rigid block resting on a rigid subsoil inclined at α, Fig. 4. Own weight force Q is split into the normal force N and the shear force T acting on the base of the block. For simplicity, it is assumed that the base acceleration A_s acts in the $\alpha - \alpha$ plane and causes the inertia force F_{as} with the opposite direction according to Newton's second law:

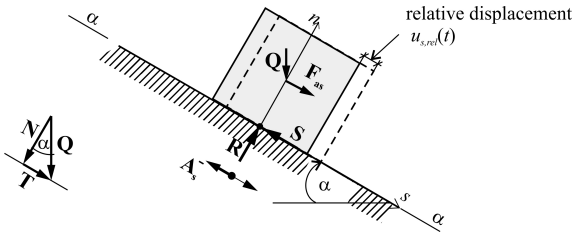

Fig. 4. Scheme of a simple system loaded by acceleration $A_s(t)$ in the $\alpha - \alpha$ plane.

$$F_{as} = m_b a_s, \tag{1}$$

where m_b denotes the mass of the block.

The reaction of the base to the above forces consists of the normal strength R and the shear strength S. The shear strength is assumed to follow the friction condition with the coefficient μ

$$S = \mu R. \tag{2}$$

The local co-ordinate system **s** is fixed in the middle point of the block before shaking. The force equilibrium shows that the maximum driving force acting on the block in the $\alpha - \alpha$ plane depends on the acceleration direction. It is determined by the shear strength (always opposite to the dynamic shear force) and the static shear force

$$F_{as} = \begin{cases} \mu N + T & \text{for} \quad A_s(t) > 0 \\ \mu N - T & \text{for} \quad A_s(t) < 0. \end{cases} \tag{3}$$

The above can be rewritten as:

$$A_s(t) > g\left(\mu \cos\alpha + \sin\alpha\right), \tag{4}$$

$$A_s(t) < -g\left(\mu \cos\alpha - \sin\alpha\right). \tag{5}$$

When one of the above conditions is met, the relative movement of the block begins. Relative displacement of the block is calculated with respect to the displacement of the base, and it is positive in the case shown in Fig. 4. It is easily seen that to initiate relative downward displacement, the critical acceleration amplitude is lower than in the case of upward sliding, in which gravity sliding force must be overcome. It is also worth noting that, in this simple case, the relative motion condition is independent of mass and time.

In general, the friction coefficient μ magnitude depends on whether the body is at rest or in relative motion. For calculating the acceleration thresholds using the above equations (Eq. 4 and Eq. 5) it should be equal to static friction coefficient μ_s and for relative motion calculations equal to kinetic friction μ_k.

Given the acceleration thresholds, it is possible to solve the motion of the block by one of implicit time integration methods, for example the finite difference method.

2.2. Solving Method

For simplicity, the solution method is shown for one motion equation:

$$a\left(t\right) = M. \tag{6}$$

The finite central difference method was used to solve Eq. 6 at n discrete time points. A linear change in velocity and constant acceleration within the time interval

$(i\Delta t,\ (i+1)\,\Delta t)$ is assumed. In fact, Eq. 6 is replaced by two first-order differential equations:

$$\dot{v}\,(t) = M, \tag{7}$$

$$\dot{u}\,(t) = v\,(t)\,, \tag{8}$$

where the dot represents differentiation with respect to time. The left-hand side of the above equations is approximated by a finite difference at the discrete time $(i + 1/2)\,\Delta t$:

$$\dot{v}\,((i+1/2)\,\Delta t) = \frac{v\,((i+1)\,\Delta t) - v\,(i\Delta t)}{\Delta t}, \tag{9}$$

$$\dot{u}\,((i+1/2)\,\Delta t) = \frac{u\,((i+1)\,\Delta t) - u\,(i\Delta t)}{\Delta t}. \tag{10}$$

The adoption of the above approximations in Eq. (7) and Eq. (8) gives:

$$v\,((i+1)\,\Delta t) = \frac{a\,((i+1)\,\Delta t) + a\,((i)\,\Delta t)}{2}\Delta t + v\,(i\Delta t)\,, \tag{11}$$

$$u\,((i+1)\,\Delta t) = u\,(i\Delta t) + \frac{v\,((i+1)\,\Delta t) + v\,(i\Delta t)}{2}\Delta t. \tag{12}$$

Given the motion of the base and the block, it is possible to calculate the relative motion in the $\alpha - \alpha$ plane. Relative displacements are calculated with respect to the displacement of the subsoil, and in this case sliding downwards has a positive sign.

2.3. Example

Let us now consider the motion of a rigid block resting on a base inclined at 20°. The static and kinetic friction coefficient of the contact between the block and the base is $\mu_s = \mu_k = 0.5$. The acceleration threshold for downward sliding is -1.25 m/s^2, Eq. 5. The acceleration threshold for upward sliding is more than six times as high, amounting to 7.96 m/s^2, Eq. 4. Let us consider a cycling motion of the base in the inclined plane given by the following equation

$$A_s\,(t) = A_s sin\,(2\pi f_s t + \theta_s)\,, \tag{13}$$

where A_s denotes the amplitude of base acceleration, f_s denotes frequency [Hz], t denotes time [s] and θ_s denotes phase angle. Here, these motion parameters have been assumed as follows: $A_s = 0.31g$; $f_s = 1$ Hz; $\theta_s = \pi$. The motion of the base and the block, characterized by acceleration, velocity and displacement time-histories, is shown in Fig. 5. The relative velocity and displacement histories are shown in Fig. 6. After two cycles of motion, relative permanent displacement equals 0.27 m.

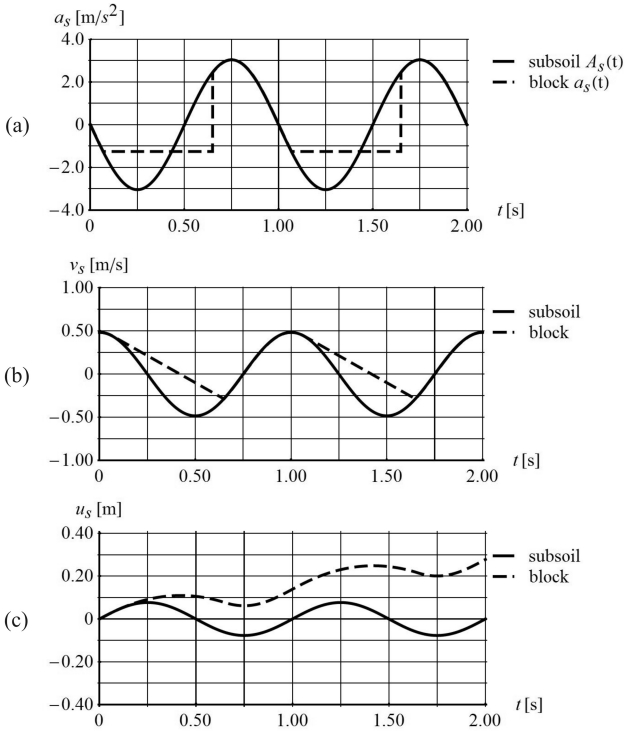

Fig. 5. Time histories of the (a) acceleration, (b) velocity, (c) displacement of the base and the block.

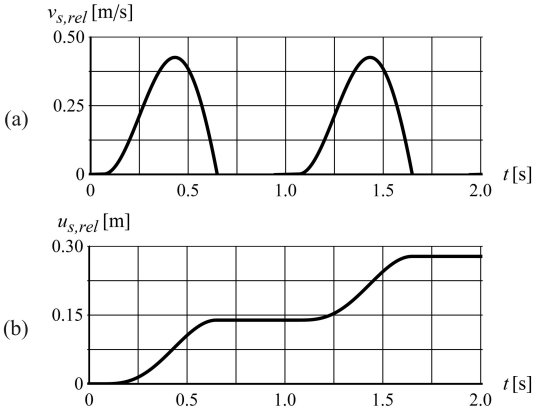

Fig. 6. Time histories of the relative (a) velocity, (b) displacement of the bloc.

2.4. Comparison of Permanent Displacement Obtained by the Proposed Method and Newmark's Approach in the Case of In-plane Acceleration

For this simple case it is also possible to calculate permanent displacement by Newmark's stability approach (Newmark 1965). There are four main steps in this method. First, the factor of safety F must be determined, which in this case is expressed by

$$FS = \frac{S}{F_{as} + T}, \tag{14}$$

where S denotes the shear strength, T denotes the static shear force, and F_{as} denotes the dynamic shear force in an "out of slope" direction. Second, the yield acceleration a_c for an assumed value of $FS = 1$ must be determined. It is calculated as the ratio of possible to mobilized stress and the mass of the block

$$a_c = \frac{S - T}{m_b} = \mu g \cos\alpha - g \sin\alpha. \tag{15}$$

Newmark's approach considers only downward displacement, so there is only one condition which corresponds to downwards sliding. Because the direction of inertia forces is opposite to that of acceleration, for the left-to-right sliding and the co-ordinate axes considered, the threshold is a_c equal -1.25 m/s^2. In the third step, the relative velocities are calculated by numerical integration of the parts of acceleration time-history which exceed the threshold a_c determined, Fig. 7. It should be noted, that the integration is continued until the block stops. Then, in the last step, relative displacements are calculated on the basis of relative velocities. After two cycles, the cumulative relative displacement is 0.278 m, which is almost the same as the value obtained by the finite difference method.

3. Rigid Block Affected by Horizontal and Vertical Accelerations

Let us now consider a simple system of two rigid bodies, consisting of a rigid block resting on a rigid base inclined at α, loaded by inertia forces F induced by both horizontal and vertical base accelerations, Fig. 8. It was assumed that the positive subsoil accelerations A_x and A_y cause an inertia forces:

$$F_{ax} = m_b a_x, \tag{16}$$

$$F_{ay} = m_b a_y, \tag{17}$$

where a_x and a_y denote the horizontal and vertical accelerations of the block, respectively. Also in this case the force equilibrium has been analyzed in the local coordinate system (s, n), thus all the forces are projected on directions: normal and tangential to the slip plane $\alpha - \alpha$. The inertia forces are decomposed into normal components F_{nx}, F_{ny} and tangent components F_{sx}, F_{sy} on an $\alpha - \alpha$ plane. Their dependence on the

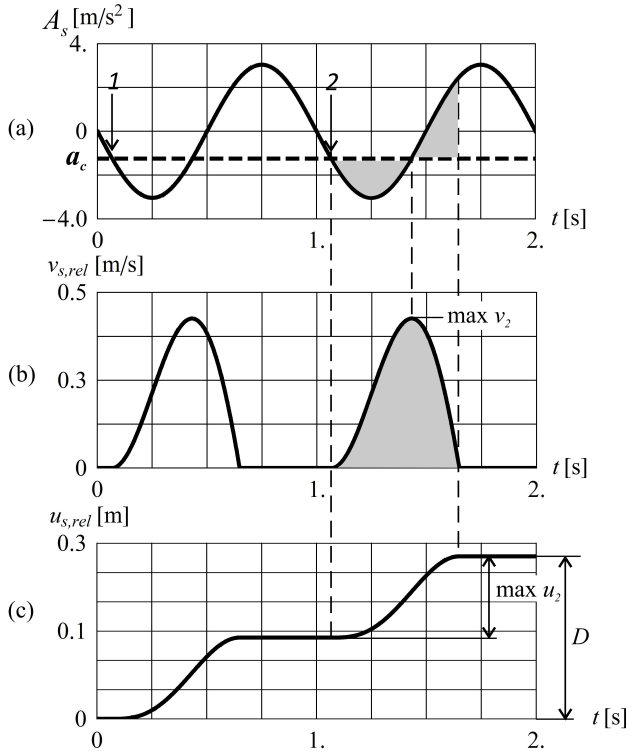

Fig. 7. (a) The time history of the acceleration of the base and the yield acceleration in the $\alpha - \alpha$ plane, (b) the time history of the relative velocity of the block, (c) the time history of the relative permanent displacement of the block.

slope inclination is shown in Fig. 9. In the case of a small slope inclination, the dominant part of the driving force is horizontal acceleration, and the dominant component affecting the shear strength is vertical acceleration.

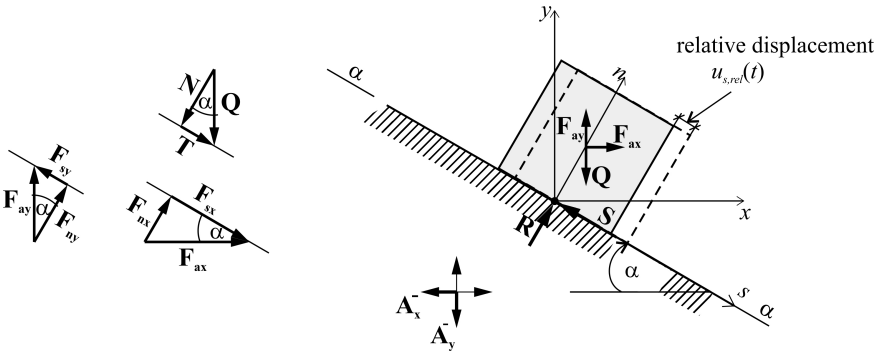

Fig. 8. Scheme of a simple system loaded by horizontal $A_x(T)$ and vertical $A_y(T)$ accelerations.

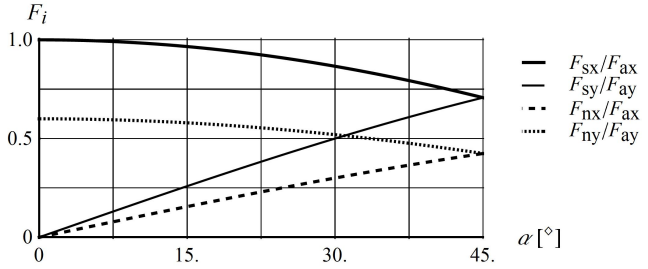

Fig. 9. The dependence of inertia forces on slope inclination for friction coefficient $\mu = 0.6$ and the same acceleration amplitude.

The driving motion of the base in the inclined plane is defined by the following equations:

$$A_s(t) = A_x(t)\cos\alpha - A_y(t)\sin\alpha, \tag{18}$$

$$A_n(t) = A_x(t)\sin\alpha + A_y(t)\cos\alpha. \tag{19}$$

Inertia forces $\boldsymbol{Fas}$ and $\boldsymbol{Fan}$ at time t_1 acting on the block resting on inclined plane affected by resultant of exemplary harmonic horizontal and vertical acceleration $\boldsymbol{A_1}$ are shown in Fig. 10. Both above-mentioned forces have negative impact on block stability, the sliding force is increased by F_{as} and the shear strength is reduced by F_{an}, respectively.

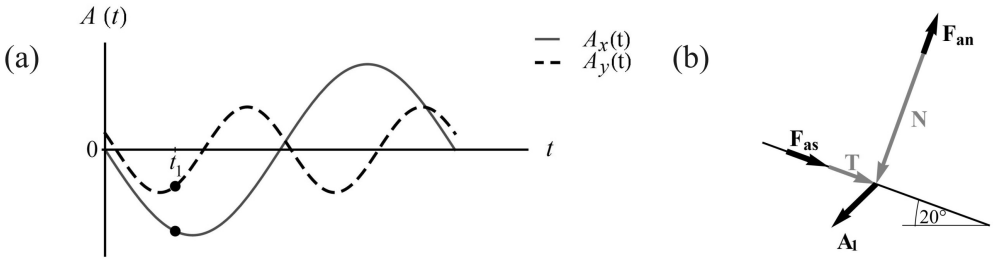

Fig. 10. (a) Exemplary harmonic horizontal and vertical acceleration time-histories, (b) dynamic forces acting on the block resting on inclined base loaded by acceleration $\boldsymbol{A}_1$ at time t_1.

It is assumed that the normal part of the acceleration $A_n(t)$ is well beyond the value that could cause the separation of the system. Thus

$$a_n(t) = A_n(t). \tag{20}$$

The same is assumed for the normal component that affects the shear strength S of the interface between the base and the block. Now, shear strength S depends on

the normal components of both static force S_s and dynamic force $S_d(t)$ thus it is time dependent

$$S(t) = S_s + S_d(t) = \mu N + \mu F_{nx}(t) + \mu F_{ny}(t). \tag{21}$$

The maximum driving force acting on the block in the s direction is determined by the shear strength $S(t)$ and the static shear force T. Thus, the time history of block acceleration $a_s(t)$ will be examined to determine relative displacement. The co-ordinate axes x, Fig. 8, are chosen in such a way that negative values of the accelerations A_x^- and A_y^- for the same amplitude result in the critical case of the block sliding down the slope ($F_{sx} > F_{sy}$). In that case, both accelerations decrease the slip surface strength S. The acceleration threshold for upward sliding is the combination of A_x^+, A_y^-. However, the exact critical condition for sliding depends on the slope inclination α, friction coefficient μ, acceleration amplitude and, last but not least, vertical acceleration frequency. The force equilibrium in the $\alpha - \alpha$ plane, covering all possible force combinations, is expressed by

$$F_{as} = \begin{cases} \mu(N + F_{nx} + F_{ny}) + T & \text{for} \quad A_x > 0 \ \text{ and } \ A_y > 0 \\ \mu(N + F_{nx} - F_{ny}) + T & \text{for} \quad A_x > 0 \ \text{ and } \ A_y < 0 \\ \mu(N - F_{nx} + F_{ny}) - T & \text{for} \quad A_x < 0 \ \text{ and } \ A_y > 0 \\ \mu(N - F_{nx} - F_{ny}) - T & \text{for} \quad A_x < 0 \ \text{ and } \ A_y < 0. \end{cases} \tag{22}$$

After making use of an appropriate trigonometric identity in Eq. 21 and acceleration signs, one can write the upward relative motion condition as

$$A_s(t) > g(\mu \cos\alpha + \sin\alpha) - \mu(A_x(t)\sin\alpha + A_y(t)\cos\alpha), \tag{23}$$

and the downward relative motion condition as

$$A_s(t) < -g(\mu \cos\alpha - \sin\alpha) - \mu(A_x(t)\sin\alpha + A_y(t)\cos\alpha). \tag{24}$$

3.1. Parametric Study in the Case of Harmonic Motion

The above given equations are valid for general form of the base acceleration functions. However, a common practice in simplified theoretical models is the replacement of the actual acceleration by equivalent harmonic or cyclic loading (Srbulov 2008) which can give opportune insight into the problem solved. Let us consider a harmonic motion of the base in both horizontal and vertical directions, given by the following equations:

$$A_x(t) = A_x sin(2\pi f_x t + \theta_x), \tag{25}$$

$$A_y(t) = A_y sin(2\pi f_y t + \theta_y), \tag{26}$$

where A denotes the amplitude of base acceleration, f denotes frequency, t denotes time, and θ denotes phase angle in the direction given in the subscript.

3.1.1. Critical Phase Angle of Vertical Acceleration

The influence of the vertical acceleration frequency f_y on permanent displacement has been proved in calculation. Comparison of subsoil and block accelerations time-histories for two different frequencies of vertical harmonic loading have been shown in Fig. 11. It has been revealed that vertical loading characterised by higher frequency is less severe for rigid block stability, Fig. 12. The vertical motion with the frequency of 4 Hz caused about 30% lower permanent displacement than for the case of vertical motion with the frequency of 1 Hz.

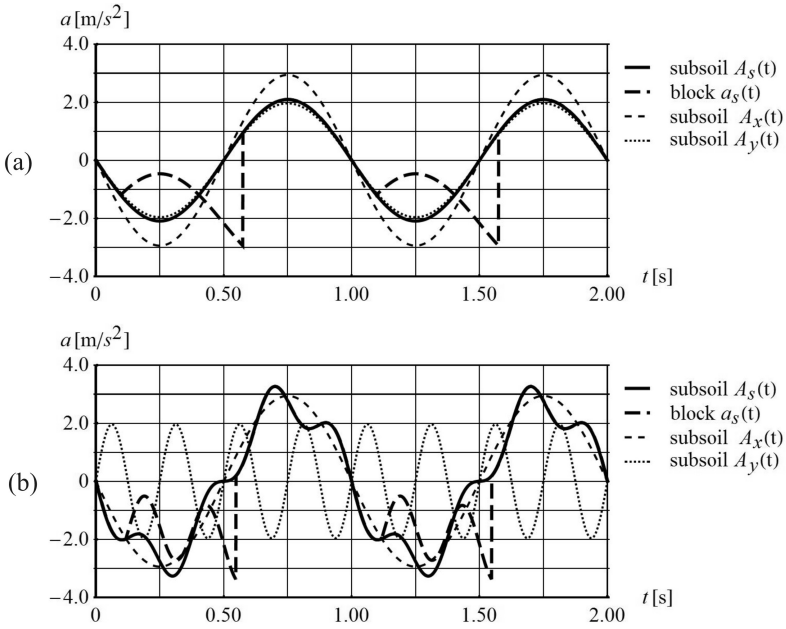

Fig. 11. Comparison of subsoil and block accelerations time histories acting along $\alpha = 20°$ inclined slip surface with $\mu_s = \mu_k = 0.6$ driven by subsoil horizontal acceleration of amplitude $A_x = 0.3g$, frequencies $f_x = 1$ Hz, phase angles $\theta_x = \pi$ and vertical acceleration (a) $A_y = 0.2g$, $f_y = 1$ Hz, $\theta_y = \pi$, (b) $A_y = 0.2g$, $f_y = 4$ Hz, $\theta_y = 0$.

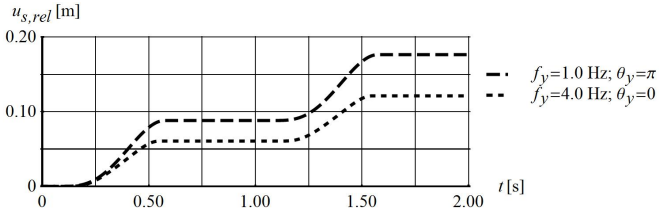

Fig. 12. Comparison of the block relative displacement for different vertical motion (data given in Fig. 11)

However, this relationship must be considered simultaneously with the vertical motion phase angle θ_y. A comparison of relative velocities and displacement time histories caused by three examples of base acceleration time histories differing only in θ_y is shown in Fig. 13. The parametric study was carried out with respect to the horizontal frequency $f_x = 1$ Hz and the phase angle $\theta_x = \pi$.

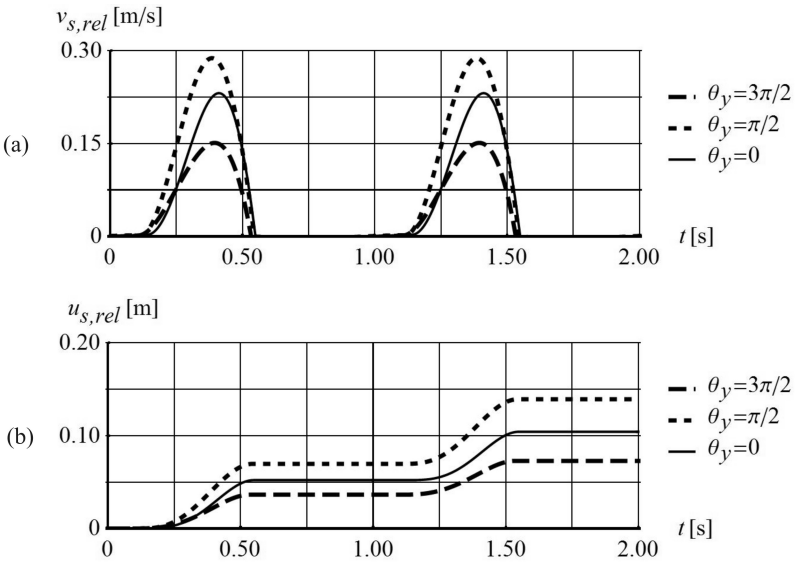

Fig. 13. Comparison of the (a) relative velocity and (b) relative displacement caused by harmonic loading $A_x = 0.3g$, $A_y = 0.2g$, $f_x = 1$ Hz, $f_y = 2$ Hz, $\theta_x = \pi$ and different vertical acceleration phase angles θ_y.

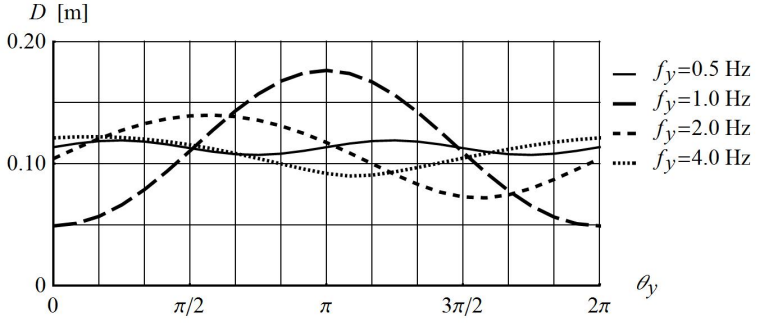

Fig. 14. Critical phase angle θ_y of harmonic vertical base motion for a rigid block resting on a slope inclined at $\alpha = 20°$ with $\mu_s = \mu_k = 0.6$ and loaded by harmonic motion$A_x = 0.3g$, $A_y = 0.2g$, $f_x = 1$ Hz, $\theta_x = \pi$.

Having reavealed this relationship critical phase angles have been determined for six frequencies of vertical acceleration. The results for bases inclined at the angle of

20° are presented in Fig. 14. The greatest effect of the vertical component of acceleration was obtained for a frequency compatible with the frequency of the horizontal component of acceleration and compatible phases. The impact of the phase angle for the permanent displacement decreases with increasing frequency. However, even for a frequency four times the frequency of the horizontal oscillation, these differences are noticeable and equal to 33%. The same test was performed for different vertical acceleration amplitudes A_y, slope inclinations and static friction coefficients μ_s, which confirmed the above conclusions.

3.1.2. Influence of the Kinetic Friction Coefficient on Permanent Displacement

It is obvious that the friction coefficient has an impact on acceleration thresholds, so these results are not shown. However, the distinction between static μ_s and kinetic friction μ_k has a significant influence on the assessment of permanent displacement. After relative motion has been initiated, friction between bodies decreases. Lower friction results in a slower braking and extension of time during which the block moves separately. The calculations have been performed for the same harmonic motion but two different kinetic friction coefficient magnitudes. The comparison of block acceleration time histories and the relative displacements are shown in Fig. 15. A 10% decrease in the friction coefficient from 0.60 to 0.54 results in 61.8% higher relative permanent displacement after two cycles of motion. It is obvious that the difference is greater for lower magnitude of kinetic friction coefficients.

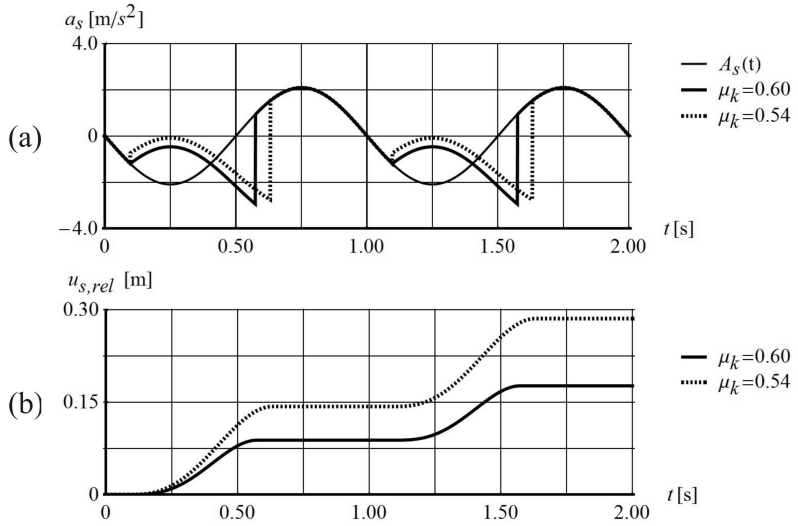

Fig. 15. Comparison of (a) accelerations acting in slip plane, (b) relative displacement of a rigid block on a base inclined at $\alpha = 20°$ for two kinetic friction coefficient magnitudes μ_k ($A_x = 0.3g$, $A_y = 0.2g$, $f_x = f_y = 1$ Hz, $\theta_x = \theta_y = \pi$).

3.2. Comparison of Permanent Displacement Obtained by the Proposed Method and Newmark's Approach in the Case of Horizontal Acceleration

Let us now compare permanent displacement in the case of the slip surface strength calculated for static and dynamic forces, and for only static forces, labelled $S(A)$ and S = const respectively. The results for a rigid block resting on a base inclined at 20° loaded by harmonic accelerations in phase with amplitudes $A_x = 0.3g$ and $A_y = 0.1g$ and frequencies $f_x = f_y = 1$ Hz are shown in Fig. 16. After two cycles, permanent displacement for the strength dependent on the dynamic forces is equal 0.36 m and is more than two times as large as it is for the constant strength case.

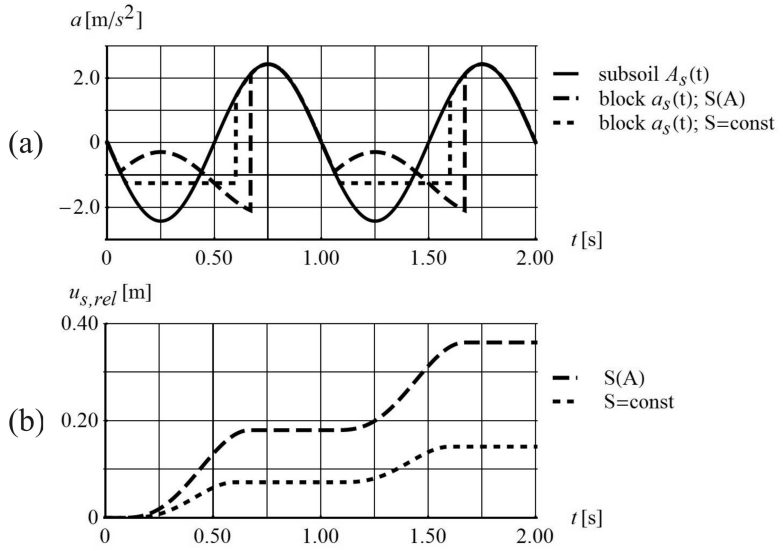

Fig. 16. Comparison of the (a) acceleration and (b) relative motion for the slip surface strength affected and unaffected by normal components of subsoil accelerations ($A_x = 0.3g$, $A_y = 0.1g$, $f_x = f_y = 1$ Hz, $\theta_x = \theta_y = \pi$)

Let us consider a rigid block resting on a base inclined at 20° loaded by a harmonic horizontal acceleration with an amplitude of $0.33g$, which gives $0.31g$ in the $\alpha - \alpha$ plane, as in Section 2.3. Let us recall that, according to Newmark's approach, the permanent displacement after two cycles was 0.28 m. The influence of the normal component of acceleration increased the permanent displacement to 0.41 m, Fig. 17.

4. Permanent Displacement in Cases of Recorded Acceleration Time Histories

The proposed method was applied for stability assessment in cases of various recorded acceleration time histories. In the paper, the well-known *El Centro* time history is examined. Three perpendicular components of acceleration were recorded in time:

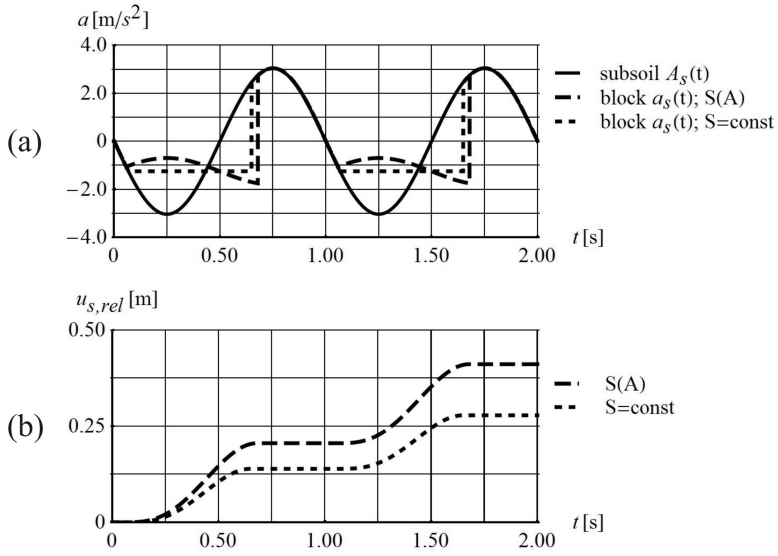

Fig. 17. Comparison of the (a) acceleration and (b) relative motion for the slip surface strength affected and unaffected by normal components of subsoil accelerations ($A_x = 0.33g$, $A_y = 0g$, $f_x = f_y = 1$ Hz, $\alpha = 20°$ and $\mu_s = \mu_k = 0.5$)

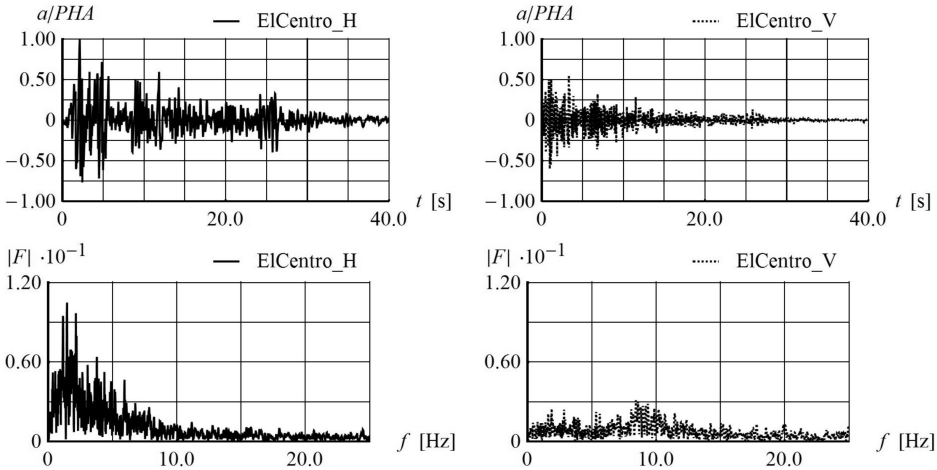

Fig. 18. Time histories of (a) the horizontal – H and (b) vertical – V acceleration components registered at a distance of 15 km from the epicentre of the 6.5 local magnitude *El Centro* earthquake, USA 1940 (in 0.2 to 25 Hz frequency band), (c), (d) their respective Fourier acceleration spectra.

East-West, North-South and vertical, Fig. 18. The peak ground acceleration and Arias intensity are higher for the North-South direction. Thus, this signal was chosen as the horizontal component of acceleration H. The calculated percentage ratio of the peak accelerations (vertical to horizontal) within the 25 Hz frequency band is equal to 60%.

The peak horizontal ground acceleration PHA was $0.3g$, which allowed to conduct comparative calculations. The relative displacement history calculated on the basis of the proposed model compared with that calculated by Newmark's method is shown in Fig. 19. It shows 66% increase in permanent displacements D taking into account the impact of dynamic forces on the slip surface strength.

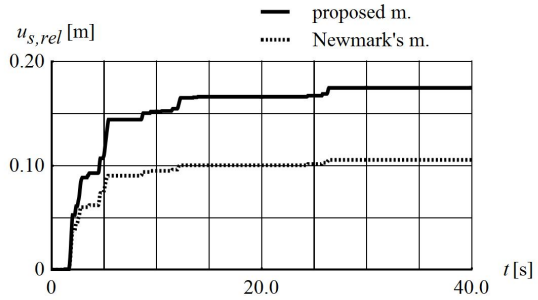

Fig. 19. Comparison of the relative motion of a rigid block on a slope inclined at $\alpha = 20°$ with $\mu_s = \mu_k = 0.46$ affected by the *El Centro* earthquake with the peak values $PHA = 0.3g$ and $PVA = 0.6PHA$ calculated by the proposed method and Newmark's method.

5. Conclusions

The stability analysis for a rigid earth structure was proposed, using a time-dependent limit equilibrium equation along the slip surface of a potentially sliding mass. Some obvious conclusions from the equations derived, consistent with intuition, show that the most critical downward sliding is caused by the horizontal base acceleration acting in the opposite direction, and that the amplitude of the acceleration needed to cause downward sliding is lower than that needed for upward sliding. Sliding on a slope is, for the most part, driven by the shear component of horizontal acceleration, but the normal component that strongly affects the interface shear strength comes from vertical acceleration.

Some cases of harmonic and real earthquake accelerations were considered. The results show that the effect of the normal component on the interface shear strength should not be neglected even for the case of horizontal acceleration. In the *El Centro* excitation considered here, Newmark's method, commonly used for stability assessment, yields permanent displacements smaller by as much as 40%.

The most important conclusions of the parametric analysis conducted on harmonic motion are as follows:

1. The interface strength highly depends on the vertical acceleration frequency;
2. The critical phase angle was found to be frequency dependent;
3. The impact of vertical acceleration on stability decreases with the increasing frequency ratio f_y/f_x.

Acknowledgments

Calculations were carried out at the Academic Computer Centre in Gdańsk.

References

Amorosi A., Boldini D., Elia G. (2010) Parametric study on seismic ground response by finite element modeling, *Comp Geotech*, **34**, 515–528.

Ambraseys N. N., Sarma S. K. (1967) The response of earth dams to strong earthquakes, *Geotechnique*, **17** (3), 181–213.

Biondi G., Cascone E., Maugeri M. (2002) Flow and deformation failure of sandy slopes, *Soil Dyn Earthq Eng*, **22**, 1103–1114.

Bray J. D., Travasarou T. (2007) Simplified procedure for estimating earthquake-induced deviatoric slope displacement, *J Geotech Geoenviron Eng* ASCE, **133** (4), 381–392.

Clough R. W., Chopra A. K. (1966) Earthquake stress analysis in earth dams, *J Eng Mech Division*, ASCE, **92** (EM2), 197–211.

Day R. T. (2002) *Geotechnical earthquake engineering handbook*, McGraw-Hill.

Dobry R. (2014) Simplified methods in Soil Dynamics, *Soil Dyn Earthq Eng*, **61–62**, 246–268.

Dulińska J. (2012) *Ziemne budowle hydrotechniczne na terenach sejsmicznych i parasejsmicznych w Polsce. Wybrane aspekty modelowania i obliczeń*, (Water earth structures in seismic and paraseismic areas in Poland. Selected aspects of modeling and calculations), Wydawnictwo Politechniki Krakowskiej, Kraków (in Polish).

Duncan J. (1996) State of the art: limit equilibrium and finite-element analysis of slopes, *J Geotech Engrg*, ASCE, **122** (7), 577–596.

Eurocode 8. EN 1998:2004. *Design of structures for earthquake resistance* (Part 1, Part 5).

Feng Z., Tsai P. H., Li J. N. (2010) Numerical earthquake response analysis of the Liyutan earth dam in Taiwan, *Nat Hazards Earth Syst Sc*,**10**, 1269–1280.

Gazetas G., Garini E., Anastasopoulos I., Georgarakos T. (2009) Effects of near-fault ground shaking on sliding systems, *Journal of Geotechnical and Geoenvironmental Engineering*, ASCE, **135** (12), 1906–1920.

GEO-SLOPE International Ltd. 2010 *Dynamic Modeling with QUAKE/W 2007. An Engineering Methodology*.

Hynes-Griffin M. E., Franklin A. G. (1984) *Rationalizing the seismic coefficient method*, Miscellaneous Paper, GL-84-13. US Army Engineers Waterways Experiment Station. Geotechnical Laboratory. Vicksburg, Mississippi.

Ishibashi I., Zhang X. (1993) Unified dynamic shear moduli and damping ratios of sand and clay, *Soils Found*, JGS, **33** (1), 182–191.

Ishihara K. (2003) *Soil Behaviour in Earthquake Geotechnics*, Clarendon Press, Oxford.

Jibson R. W. (1993) Predicting earthquake-induced landslide displacement using Newmark's sliding block analysis, *Transp Res*, 1411, 9–17.

Jibson R. W. (2011) Methods for assessing the stability of slopes during earthquakes – A retrospective, *Eng Geology*, **122**, 43–50.

Kramer S. L. (1996) *Geotechnical Earthquake Engineering*, Prentice-Hall Inc.

Makdisi F. I., Seed H. B. (1978) A simplified procedure for estimating earthquake-induced deformations in dams and embankments, *J Geotech Eng Division*, ASCE, **104** (7), 849–867.

Newmark N. M. (1965) Effects of earthquakes on dams and embankments, *Geotechnique*, **15** (2), 139–160.

Qi Sh., Liu Ch. (2015) Permanent displacement of rock slope considering degradation of slide surface during earthquake, [in:] *10th Asian Regional Conference of the International Association for Engineering Geology and the Environment*, Kyoto, Japan.

Romero R. (2000) Seismically induced landslide displacements: a predictive model, *Eng Geology*, **58**, 337–351.

Sawicki A., Chybicki W. (2005) Horizontal motion of a rigid block resting on accelerating subsoil, *Archives of Hydro-Engineering and Environmental Mechanics*, **52** (2), 147–160.

Sawicki A., Chybicki W., Kulczykowski M. (2007) Influence of vertical ground motion on seismic-induced displacements of gravity structures, *Comput Geotech*, **34**, 485–497.

Sica S., Santucci de Magistris F., Vinale F. (2002) Seismic behaviour of geotechnical structures, *Ann Geophys*, **45** (6), 799–815.

Srbulov M. (2008) *Geotechnical Earthquake Engineering. Simplified Analyses with Case Studies and Examples*, Springer.

Świdziński W., Korzec A. (2015a) Numerical modelling of the seismically induced deformation of tailings dam, [in:] *Proceedings of the XVI ECSMGE – Geotechnical Engineering for Infrastructure and Development*, ed. Winter M., Smith D. M., Eldred P. J. L. & Toll D. G. , ICE Publishing, 2189–2194.

Świdziński W., Korzec A. (2015b) Ocena dynamicznej odpowiedzi zapór ziemnych w świetle aktualnych unormowań (Current regulations of seismic stability assessment of earth dams), *Inżynieria Morska i Geotechnika*, **3**, 489–493 (in Polish).

Terzaghi K. (1950) Mechanisms of Landslides, *Eng Geol*, (Berkeley) Volume, GSA.

The European Strong-Motion Database http://www.isesd.hi.is (downloaded in 2015).

Wieland M. (2008) Large dams the first structures designed systematically against earthquakes, *The 14th World Conference on Earthquake Engineering*, China.